RESEARCH ARTICLE

WILEY

Fire and collapse: Untangling the formation of destruction layers using archaeomagnetism

Ruth Shahack-Gross[1] (iD) | Ron Shaar[2] | Erez Hassul[2] | Yael Ebert[2] | Mathilde Forget[3] | Norbert Nowaczyk[4] | Shmuel Marco[5] | Israel Finkelstein[6] | Amotz Agnon[2]

[1]Department of Maritime Civilizations, University of Haifa, Haifa, Israel

[2]Institute of Earth Science, The Hebrew University of Jerusalem, Jerusalem, Israel

[3]Fives Machining, Saint Laurent Les Tours, France

[4]GFZ German Research Centre for Geosciences, Potsdam, Germany

[5]Department of Geophysics, Tel Aviv University, Tel Aviv, Israel

[6]Institute of Archaeology, Tel Aviv University, Tel Aviv, Israel

Correspondence
Ruth Shahack-Gross, Department of Maritime Civilizations, University of Haifa, Haifa, Israel.
Email: rgross@univ.haifa.ac.il

Scientific editing by Rob Sternberg

Abstract

Historical events are sometimes expressed in destruction layers. We present here a study in which aspects of construction, destruction, and chronostratigraphy of fired mud bricks were explored using archaeomagnetism, infrared spectroscopy, and micromorphology. We measured 88 oriented samples mostly collected from one stratum, dated *ca.* 1000 B.C.E., representing a destroyed late Canaanite (late Iron Age I) city in Tel Megiddo, Israel. Firing temperatures, evaluated from infrared spectroscopy, micromorphology, and high-temperature magnetic susceptibility cycles, range between 300°C and 800°C. Samples studied in one archaeomagnetic site yield a single stable magnetization vector in demagnetization experiments. Archaeomagnetic site means of three standing walls are grouped near the expected direction of the ancient geomagnetic field. We propose that walls in the destruction layer were constructed from sun-dried mud bricks that later burned during the destruction. Collapsed bricks and tilted walls show variable directions, diagnostic for the relative timing of collapse and cooling of bricks, during and following the destruction event. In addition, we attempt to assign stratigraphic affiliation based on archaeomagnetic considerations to standing walls, which are spatially disconnected from the studied destruction layer. Altogether, this study demonstrates the usefulness of archaeomagnetism to understanding site formation processes related to fire and destruction.

KEYWORDS

archaeomagnetism, burnt mud brick walls, FTIR spectroscopy, Megiddo destruction layer, micromorphology

1 | INTRODUCTION

Destruction of settlements while they are inhabited (rather than after their abandonment) is a phenomenon globally recognized in archaeology. It is evident on a regional scale as well as on the site level, with the latter being especially known in urban centers (Torrence & Grattan, 2002). Among the various causes for destruction, conflagration is rather well identified, as it produces dramatic field evidence in ancient settlements (e.g., Regev et al., 2015; Stevanović, 1997; Twiss et al., 2008). Conflagration events result in destruction layers, often characterized by *in situ* human activity remains mixed with and/or covered by charcoal and ash. This assemblage is typically further covered by a thick layer of architectural collapse. Because such destruction events tend to be rapid, sealing material culture items and features in their place of production and use (sometimes also including trapped remains of the

inhabitants), there is greater opportunity for reliable interpretation of past life ways and intensive research into activity patterns, which can lead to understanding ancient households and broader economic and social patterns (Driessen, 2013; Torrence & Grattan, 2002).

Architectural units in urban centers representing the last 10,000 years in the ancient Near East were, in many cases, constructed from chaff-tempered sun-dried mud bricks. The virtues of this construction material have long been recognized and include its low cost, ease of access, ease of manufacture, weather-proofing and insulation qualities, ability to withstand heavy loads (multiple-storied structures), and durability against earthquake shaking (van Beek & van Beek, 2008; see also Homsher, 2012). Fired mud bricks are also prevalent in Near Eastern mound sites. They often appear in piles or wall segments; common archaeological wisdom takes this to indicate destruction by fire. Notably, new cities are often constructed above these piles, but

evidence for re-use of bricks from destruction levels has not been purported.

Recent experimental research into the effect of fire on mud bricks showed that chaff, a common component within sun-dried mud bricks, burns when bricks are heated above 400°C, elevating temperatures within the bricks to as much as 100°C above the temperature on the outside (Forget et al., 2015). This observation raises the question whether sun-dried mud bricks, despite having the many virtues outlined above, may in fact be disadvantageous in case of fire, that is, become a death-trap during conflagration events. Forget and Shahack-Gross (2016) further show that it takes a minimum of 2–3 hours of constant heat, conducted from all directions, to produce homogeneously burnt mud bricks. Therefore, the effect of fire on mud brick architectural spaces poses an interesting perspective for understanding the inter-relationship between humans and their constructed living space.

With this information at hand, and assisted with microarchaeological techniques such as infrared spectroscopy that allow assessment of burning temperatures from clay minerals, the following two opposing interpretations have been suggested for ancient construction technology: (a) homogeneously burnt mud bricks indicate construction with pre-fired bricks (e.g., Namdar et al., 2011), or (b) homogeneously burnt mud bricks indicate *in situ* burning of walls composed of sun-dried chaff-tempered mud bricks (e.g., Forget et al., 2015). Both these interpretations would be consistent with the data, but up to this point, one could not be chosen over the other because systematic geoarchaeological and experimental studies that look into this question have only begun in the last several years. Using either one of the two interpretations would lead to different historical and anthropological implications.

Considering the first interpretation—construction with pre-fired mud bricks—implies that certain archaeological layers interpreted as the result of conflagration events may have not been destroyed by fire at all. This would further influence the understanding of the level of technological skill of these ancient Near Eastern societies, and in turn reflect on work organization and human–environment interactions. In other words, using pre-fired bricks would indicate high investment in brick manufacture technology (unless people re-used fired bricks) and an environmental impact such as deforestation due to the need for large amounts of fuel material. Also, if evidence for pre-firing of bricks is revealed in Bronze and Iron Age layers, it would put the appearance of this technology earlier than generally perceived. It is noteworthy that despite years of excavations and surveys in the Near East, brick kilns dating to the Bronze and Iron Ages have not been recorded. According to the second interpretation (the prevalent one among Near Eastern archaeologists), whereby construction is with sun-dried mud bricks, the implication for the use of technology by ancient societies in the Near East would be different, indicating lower investment in brick manufacture technology and no environmental impact related to fuel requirements. In addition, it would affect the understanding about the relationship between destruction layers and historical events. Below we present a study that aims to resolve the issue of construction technology of bricks using an independent method, namely archaeomagnetism.

1.1 | Archaeomagnetism

Studies of the Earth's ancient magnetic field use a variety of materials, geological and archaeological. The working assumption that underlies archaeomagnetism is that an archaeological artifact can acquire a remanent magnetization through cooling after being heated to high temperatures, which can be stable over thousands of years. This is known as thermoremanent magnetization (TRM), a vectorial property of the artifact. Thus, *in situ* fired archaeological features carry TRM pointing to the direction of the ancient geomagnetic field at the time of the fire. The direction is expressed in terms of declination (*Dec*), the angle between the horizontal component of the vector and the geographic north, and inclination (*Inc*), the angle between the vector and the horizontal plane.

The characteristics of TRM relevant to the current study are that (a) TRM is proportional and parallel to the ambient field in which it was acquired, (b) TRM is the vectorial sum of independent partial TRMs acquired at different temperatures termed "blocking temperatures" (T_B), (c) a natural material composed of different minerals can have a broad spectrum of T_B ranging up to the Curie temperature (T_c) of the minerals, (d) partial TRM acquired at T_B is erased by re-heating the artifact to equal or higher T_B, and (e) TRM might be masked by nonthermal remanent magnetization, which we consider noise for the present purpose. Laboratory demagnetization methods are designed to recover the declination and inclination of the ancient magnetization by a series of demagnetization steps. This procedure sheds light on the processes involved in the ancient heating events (Gallet et al., 2009; Goulpeau, 1994; Hassul et al., in press; Lanos, Kovacheva, & Chauvin, 1999; Shaar et al., 2016; Sternberg, 2008; Sternberg & McGuire, 1990; Sternberg et al., 1999).

Burnt structures can theoretically supply human-related information on an archaeological event of destruction by fire. It can potentially inform about the method of construction, identify heating events that affected the archaeological material (provided that successive heating events occurred with successively lower blocking temperatures, below the maximum T_B), and untangle collapse directions of architectonic units. In addition, it can possibly resolve chronostratigraphic questions about the association of burnt walls from unclear contexts to specific destruction events. For example, Shaffer (1993) conducted an archaeomagnetic study to understand the construction and/or collapse of a wattle-and-daub Neolithic structure in Italy. He concluded that the structure burnt while walls were completely or partially standing, rather than after complete collapse. This enabled him to dismiss the hypothesis that wattle-and-daub Neolithic structures were hardened by fire prior to habitation. Goulpeau (1994) used thermal demagnetization of bricks in a Roman hypocaust to separate the partial TRM acquired when the hypocaust was used from the TRM associated with the bricks' firing. This enabled spatial reconstructions of temperatures and archaeomagnetic dating. One of the case studies in Sternberg et al. (1999), who used archaeomagnetism in several Israeli archaeological sites, was a fired mud brick from a destruction layer at Tel Miqne. It was unclear whether the brick was fired in the find place (i.e., fell and then fired) or elsewhere (i.e., fired and then fell). The archaeomagnetic analysis showed that the magnetization was acquired while the brick

cooled down in the find place. Ben-Yosef and Ron (in press) studied eight mud bricks from burnt and tilted wall segments in a destruction layer in Tel Rehov (Israel), dating to the Iron Age IIA. They identified a single heating event and concluded that the fire took place during or shortly after the tilting occurred.

Below, we present an archaeomagnetic study of mud bricks and mud brick wall segments from a well-known destruction event at Tel Megiddo (Israel). The analysis was designed to answer archaeological questions pertaining to construction with mud bricks as well as patterns of architectonic collapse during destruction. In addition, we used archaeomagnetism as a tool to determine the ages of burnt walls with unclear stratigraphic affiliation.

1.2 | Case study and research hypotheses: the destruction of Stratum VIA at Tel Megiddo, Israel

Tel Megiddo (latitude 32.58°N, longitude 35.18°E) is one of the most celebrated mound sites of the ancient world, strategically situated on the most important highway of the Near East, which led from Egypt to Mesopotamia and Anatolia (Figure 1a). It features a long history of human occupation, from the 7th or 6th millennium to the second half of the 1st millennium B.C.E. The archaeological site formed by successive construction of ancient cities one upon another, each denoted as a stratum. The current study focuses on one stratum, dating to the Late Iron Age I (late eleventh to early tenth century B.C.E.), labeled Stratum VIA by the University of Chicago team in the 1930s (Loud, 1948). According to pottery typology and other features of material culture, this stratum accords with the Canaanite tradition of the region in the late second millennium B.C.E. (Finkelstein, 2003). Following widespread exposure of this stratum across the site, it is believed that this ancient Canaanite city experienced a violent and fast destruction (Finkelstein, Ussishkin, & Halpern, 2000, 2006, 2013; Harrison, 2004; Lamon & Shipton, 1939; Loud, 1948; Schumacher, 1908; Zarzecki-Peleg, 2005). This destruction layer includes vast charred floors, with large amounts of crushed pottery vessels and other *in situ* remains, as well as several human skeletons trapped below *ca.* 1-m thick mud brick collapse. A famous marker of this stratum is the red color of its collapsed debris, interpreted to be a result of fierce fire that annihilated the city. The cause for this destruction has been debated. Two viable explanations prevail. One states that the destruction was caused by an earthquake (Cline, 2011); indeed, the city is situated close to an active tributary fault of the Dead Sea transform (Marco, 2008; Marco, Agnon, Ussishkin, & Finkelstein, 2006). The other states that the devastation was caused during a conquest (Finkelstein, 2009; Finkelstein & Piasetzky, 2009). Neither explanation is based on conclusive data, so the force behind the city's devastation remains elusive. A short occupational gap seems to have followed the destruction of Stratum VIA, based on the fact that the next phase of settlement at the site (Stratum VB) is culturally different, carrying North Israelite characteristics reflected in the ceramic traditions (and other traits of material culture) and in the layout of the city (Finkelstein, 2009; Harrison, 2004 and references therein; see Table 1 for further stratigraphic details).
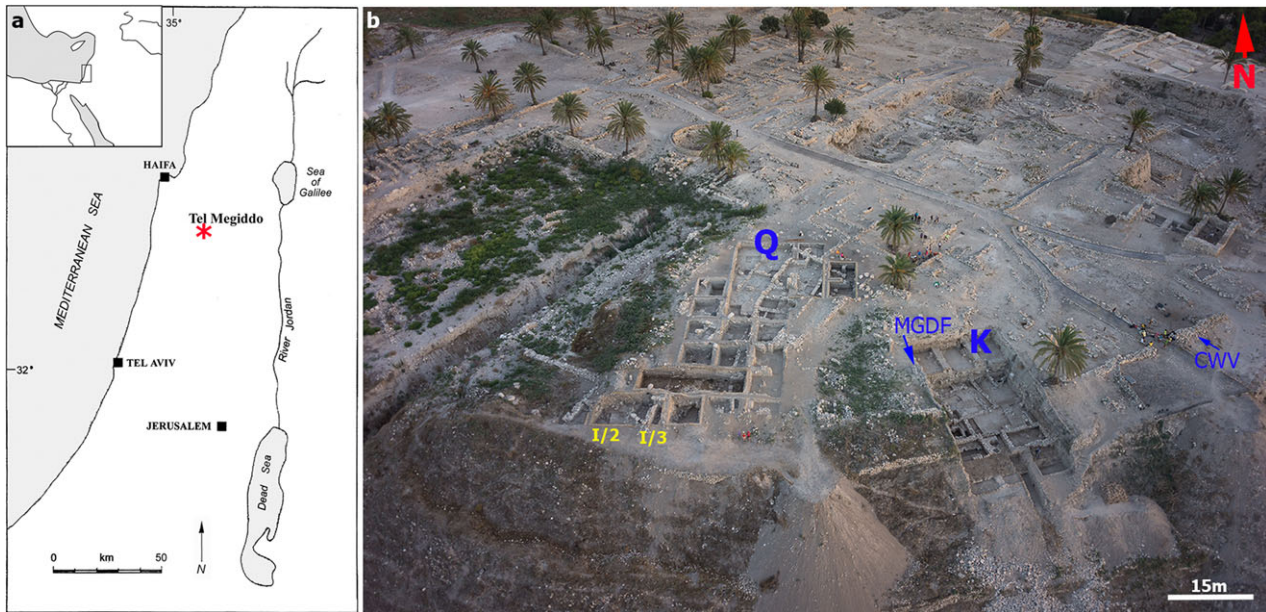
The current excavations at the site are directed by I. Finkelstein, M.J. Adams, and M.A.S. Martin. In Area Q, located on the southwestern side of the mound (Figure 1b), Late Iron Age I pottery was unearthed in association with thick and extensive piles of collapsed reddish mud bricks. Stratigraphically and ceramically this layer is indicative of Stratum VIA, locally labeled Level Q-7 (Table 1); it has been under excavation since 2012. A recent study of scattered reddish mud bricks and a wall segment in Level Q-7 utilized Fourier transform infrared spectroscopy (FTIR) and demonstrated that dozens of individual collapsed mud bricks have been homogeneously heated to roughly 600°C, whereas mud bricks in the wall segment showed a thermal gradient from about 700°C to 800°C on its edge to less than 500°C in its core (Forget et al., 2015). While the evidence from the wall segment seems to indicate that it was constructed from sun-dried mud bricks that later burnt as one unit, the homogeneous heating identified in the scattered bricks makes it unclear whether heating occurred before or after construction. The question that arises, therefore, is whether the Late Iron Age I city in Megiddo was constructed from sun-dried or pre-fired mud bricks. This case is therefore ideal to approach through archaeomagnetism because of the following reasons:

a. If walls were constructed from pre-fired bricks (prepared off-site in a kiln, extracted from the kiln and then piled to form a wall) and were not heated afterward, we would expect that archaeomagnetic directions from different bricks will be randomly scattered.

b. If walls were constructed from sun-dried bricks and heated during the destruction event, we would expect that all archaeomagnetic directions will roughly point to the reference geomagnetic field direction.

c. If walls were constructed from pre-fired bricks and later underwent another heating event at a lower temperature below the maximum unblocking temperature of the material, we would expect to identify two archaeomagnetic components with different directions: a high blocking temperature component randomly oriented and a low blocking temperature component pointing to the reference geomagnetic field direction.

d. If a wall is hot and cooling as it collapses, and then continues to cool after collapse, the alignment of TRM components in the different bricks will depend on respective blocking temperatures.

2 | MATERIALS AND METHODS

Table 2 lists the sampling locations, termed "archaeomagnetic sites" hereafter. Sample abbreviations were arbitrarily designated by one of us (E.H.) during field work. Archaeomagnetic sites from Level Q-7 include a mud-constructed cooking oven (tabun), an *in situ* standing wall consisting of eight burnt mud bricks (of which five were sampled for archaeomagnetism; MGD-A-E), and six different segments of tilted and collapsed walls found near the standing wall (one to three bricks sampled in each segment). All these were sampled during the 2012 and 2014 excavation seasons from squares I/2 and I/3 over a total area of *ca.* 50 m² (Figure 2). Two standing walls located outside area Q (labeled MGDF and CWV; Figure 1b), unearthed by the Chicago Expedition during the 1940s and left on the Tel's surface intact, were sampled as well.

FIGURE 1 (a) Map showing the location of Tel Megiddo. (b) An oblique aerial photograph of the southeastern part of the mound looking northwest, showing excavation areas Q and K, the location of excavation squares I/2 and I/3 within Area Q, and the location of two upright standing mud brick walls that were sampled outside excavation areas (MGDF and CWV), the chronostratigraphic association of which is uncertain [Color figure can be viewed at wileyonlinelibrary.com]

TABLE 1 Outline of the relative and absolute chronological scheme in Area Q at Tel Megiddo

Stratum	Relative Age	Numerical Age	Level in Area Q
IVA	Iron IIB	Eighth century B.C.E.	Q-2
VA/IVB	Late Iron IIA	First half of ninth century B.C.E.	Q-4
VB/VA-IVB transition	Early/Late Iron IIA transition	*ca.* 900 B.C.E.	Q-5
VB	Early Iron IIA	Late tenth century B.C.E.	Q-6
VIA	Late Iron I	Late eleventh to early tenth century B.C.E.	Q-7
VIB	Early Iron I	Eleventh century B.C.E.	Q-8
VIIA	Late Bronze III	Twelfth century B.C.E.	Q-9

Stratum relates to the basic nomenclature used by the University of Chicago Expedition (Loud, 1948), indicating site-wide exposure of one ancient city from a specific time period. Relative age is estimated based on pottery typology, and numerical age is based on radiocarbon determinations (see references in the text). The archaeological levels excavated in Area Q correlate typologically with the site-wide strata, with Level Q-7 being part of the city identified as the Late Iron Age I, i.e., Stratum VIA (highlighted in bold).

This was in an attempt to use their magnetic properties as chronostratigraphic markers or, more specifically, to test whether they may also belong to the Stratum VIA destruction event. Figure 3 shows the archaeomagnetic sites as they appeared in the field.

Each archaeomagnetic site was sampled through the collection of 4–21 oriented samples. Two sites were sampled using an electrical portable core 1-in. drill (MGD-A-E and MGDF) and Pomeroy orienting device. All other archaeomagnetic sites were sampled as separate blocks by marking the orientation and attitude (dip, dip-direction) on flat surfaces before removing the blocks. In the laboratory, the blocks were cut to standard archaeomagnetic size samples (2.2 cm × 2.2 cm × 1.8 cm). A total of 88 samples were prepared and measured.

Demagnetization experiments were carried out in the paleomagnetic laboratory of the Institute of Earth Sciences, the Hebrew University of Jerusalem, and in the paleomagnetic laboratory in Helmholtz

Centre Potsdam, GFZ Germany, each equipped with a three-axis 2G cryogenic magnetometer. Eighty-five samples were demagnetized under alternating field (AF) in multiple steps at progressively elevated peak fields. In addition, three samples from wall segment MGDF underwent thermal demagnetization (TH) experiments at progressively elevated temperature steps up to 590°C or until the remanent magnetization was removed. Samples for this analysis were available only from wall MGDF. The magnetization after each step was measured and plotted on an orthogonal vector end-point Zijderveld plot (Zijderveld, 1967). Best-fit directions were calculated using principal component analysis (Kirschvink, 1980). Archaeomagnetic site means were calculated using Fisher statistics (Fisher, 1953). The reliability of the mean was evaluated from the precision parameter, *k* (Fisher, 1953), a measure of the scatter of the data around the mean, and the α_{95}, the 95% confidence cone around the mean. Data were analyzed using the Demag-GUI program, part of the PmagPy v.3.9 software package

TABLE 2 List of archaeomagnetic sampling sites, with archaeological context, temperature estimation from FTIR analysis, and method of sampling

Archaeomagnetic site	Location	Description	Position	Temperature according to FTIR spectroscopy	Sampling method
MGD-A-E	Area Q, Level Q-7; Square I/3; Locus 12/Q/204	Five bricks from a standing wall segment	*In situ*, bricks lie horizontally on their wide face	500–600°C	Cores
MGD-G	Area Q, Level Q-7; Square I/2; Locus 12/Q/184	Single brick	Tilted, not *in situ*	500–600°C	Hand samples
MGD-H-I	Area Q, Level Q-7; Square I/2; Locus 12/Q/184	Two bricks from a collapsed wall segment	Tilted, not *in situ*	500–600°C	Hand samples
MGD-J	Area Q, Level Q-7; Square I/2; Locus 12/Q/184	Single brick	Tilted, not *in situ*	500–600°C	Hand samples
MTQK	Area Q, Level Q-7; Square I/2; Locus 12/Q/210	Cooking oven (tabun)	Upright oven walls, *in situ*	600–700°C	Hand samples
IBW	Area Q, Level Q-7; Square I/2-3; Locus 14/Q/068	Three bricks from a collapsed wall segment	Tilted, not *in situ*	<500–800°C	Hand samples
MCW	Area Q, Level Q-7; Square I/2-H/2; Locus 14/Q/056	Three bricks from a collapsed wall segment	Tilted, not *in situ*	700–800°C	Hand samples
MGDF	Stratigraphic affiliation is unknown	Ten bricks from a standing wall outside Area Q	Horizontal, *in situ*	700–800°C	Cores and hand samples
CWV	Stratigraphic affiliation is unknown	Three bricks from a standing wall outside Area Q	Horizontal, *in situ*	500–600°C	Hand samples

FIGURE 2 Aerial photograph of the southern part of Area Q at the end of the 2014 season, showing excavation squares I/2 and I/3 and the paleomagnetic sampling sites specific to the Late Iron Age I destruction at Level Q-7. The flat, lowest levels exposed in the sampled excavation squares and those to their east and north, correspond to the floor of Level Q-7 (correlative to the floor of Stratum VIA) [Color figure can be viewed at wileyonlinelibrary.com]

(Tauxe et al., 2016). High-temperature susceptibility cycles, an additional method that allows estimation of the temperature of the ancient heating, was measured on three samples from wall MGDF using an AGICO MFK1 kappabridge with a C4 furnace. Six heating–cooling cycles were carried out at progressively elevated peak temperatures, from 200°C to 700°C in 100°C steps, to detect alteration temperatures of the magnetic minerals upon heating. The highest temperature until thermomagnetic curves are still reversible is interpreted as a lower bound of ancient heating temperatures.

In order to further understand the material under study, we characterized the mud bricks from most archaeomagnetic sites using micromorphology and determined the temperature range to which the clay minerals within the mud bricks had been exposed, using FTIR spectroscopy. Samples cover the variety of brick colors observed in the field. Samples were analyzed with the KBr FTIR method (Weiner, 2010), using a Nicolet iS5 spectrometer (Thermo Scientific) and Omnic Software. Spectra were collected between 4000 and 400 cm^{-1} at 4 cm^{-1} resolution. Data interpretation followed the model presented

FIGURE 3 Specific sampling sites. (a) Upright standing wall segment MGD-A-E, noting the five bricks sampled from the base of this wall. (b) Upright standing wall segment MGDF. Note the variety of mud brick colors and textures (hence compositions). (c) Collapsed single-brick MGD-G after sawing and removing an oriented block sample. Note the heterogeneous composition of the brick. (d) Collapsed wall segment MGD-H-I, of which two attached bricks (H and I) have been sampled. (e) Collapsed single-brick MGD-J. (f) Collapsed wall segment IBW. (g) Collapsed wall segment MCW. (h) Upright standing wall segment CWV. Scale bar is 20 cm, except for (f) where it is 15 cm [Color figure can be viewed at wileyonlinelibrary.com]
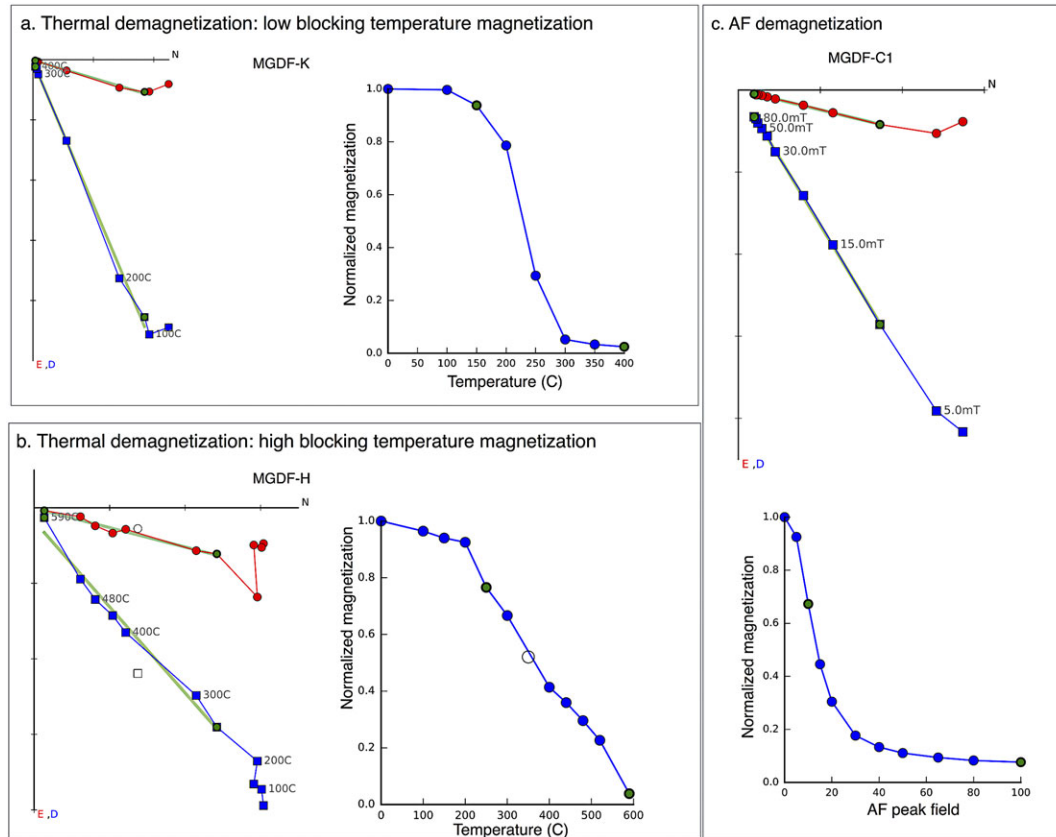
in Forget et al. (2015), showing that infrared analysis of heated calcitic-clay as found in Megiddo's mud bricks makes it possible to determine and distinguish between the following heat ranges: below 500°C, 500–600°C, 700–800°C, and above 900°C. Blocks of sampled mud bricks have been impregnated by polyester resin and prepared as 30-μm thin sections at Arizona Quality Thin Sections, Tucson, Arizona. Micromorphological observations were obtained with a Nikon Eclipse 50i POL at X2 to X400 magnifications. Descriptions follow Stoops (2003).

3 | RESULTS

3.1 | Archaeomagnetic analysis

Figure 4 shows behaviors in the AF and TH demagnetization experiments (see additional plots in the Supplementary Figure 1). All the Zijderveld plots show straight lines converging to the origin. Best-fit lines calculated using at least five points show MAD (maximum

FIGURE 4 Representative results of thermal (a, b) and AF (c) demagnetization experiment displayed on an orthogonal vector endpoint Zijderveld plot and normalized magnetization versus step. Red circles are declination and blue squares are inclination. All Zijderveld plots show straight lines converging to the origin indicating a stable single-component magnetization [Color figure can be viewed at wileyonlinelibrary.com]
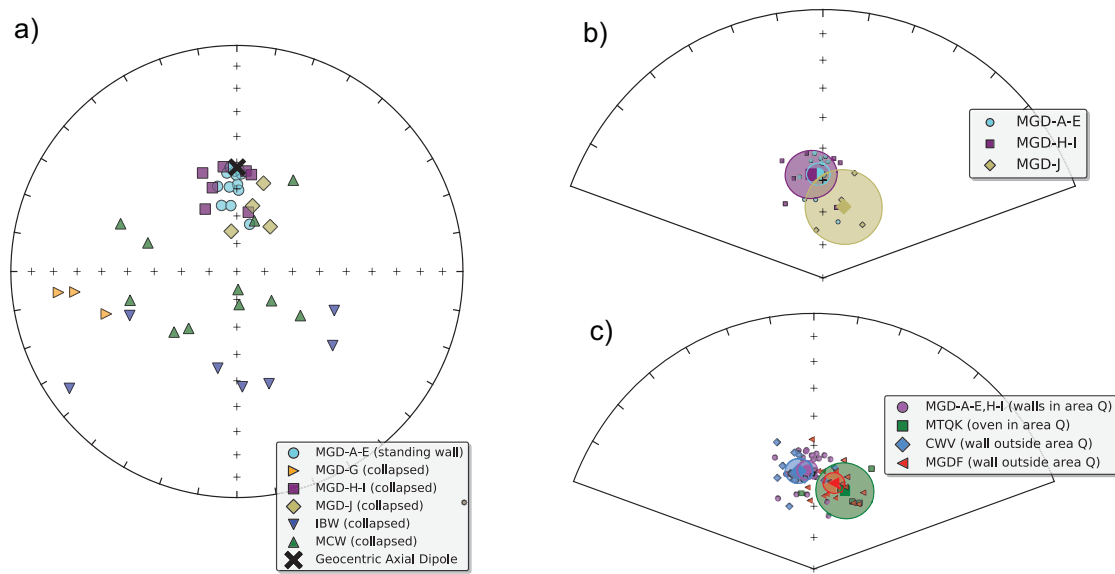
TABLE 3 Archaeomagnetic site means

Archaeomagnetic site	Declination	Inclination	n/n_0	α_{95}	k
MGD-A-E	358	58	14/16	3.4	135
MGD-H-I	353	58	7/9	7.6	75
MGD-J	016	67	4/4	11.5	65
MGDA-E,H-I,J	359	60	25/29	3.4	74
MGD-A-E, H-I	356	58	21/25	3.1	104
MTQK	022	63	5/5	9.0	72
MGDF	013	62	17/19	3.4	112
CWV	349	61	14/16	5.2	58

angular deviation; Kirschvink, 1980) lower than 5°, an indication for a single stable magnetization vector. A small (<10% of the NRM) low-temperature secondary component removed under 5 mT or 200°C is observed in some samples. We interpret this low-coercivity low-temperature component as viscous remanent magnetization (VRM) overprint. In the thermal experiments, the magnetization is almost entirely removed at 300°C or at 590°C, indicating maximum respective blocking temperatures (T_B) (Figure 4a,b). From a total of 88 samples, eight were excluded from further analysis (Table 3) on the basis of anomalous outlier directions, most likely caused by unreliable field orientation measurements or instability of the sampled material. Outlier directions were rejected when the following conditions were met: (1) the angle between the sample's archaeomagnetic direction and site's

mean was larger than $2\alpha_{95}$ and/or larger than 15°, and (2) a technical difficulty was reported for precisely measuring the field orientation of the sample.

Figure 4a shows that at least one brick holds TRM that is nearly entirely erased at 300°C. This implies that perhaps the heating was lower than 300°C. To test this possibility, we gave the samples with the low T_B a new laboratory TRM in 600°C and 50 μT in the z-axis direction of the sample. After measuring the magnetization, we gave the sample a second laboratory TRM at 300°C, this time in the x-axis direction. We carried out an AF demagnetization sequence, similar to the one shown in Figure 4 to see if we can identify two orthogonal magnetization vectors. The difference between the two TRMs was less than 2%, and the AF demagnetization revealed a single component in the x-axis

FIGURE 5 Equal area projections showing archaeomagnetic directions. (a) All samples from the different walls segments (archaeomagnetic sites) in Level Q-7. The 'x' shows the geocentric axial dipole (GAD) field direction. Three sites are grouped near the GAD direction indicating that the position of the bricks did not change since the last heating. Site means are shown in (b). (c) Archaeomagnetic site mean vectors, with Level Q-7 represented by "MGD-A-E, H-I" (see text for details), oven MTQK from Level Q-7, and the two walls with unclear stratigraphic association (CWV and MGDF). [Color figure can be viewed at wileyonlinelibrary.com]

direction. The results of this experiment indicate that the magnetization of the brick was removed at 300°C not because the heating temperature was 300°C, but because the maximal T_B of the material is 300°C.

Figure 5a shows archaeomagnetic directions of all mud brick samples collected from Level Q-7, including one standing wall and several collapsed wall segments. The reference archaeomagnetic direction at the time of the heating is unknown, thus the geocentric axial dipole (GAD) direction (dec = 0°, inc = 52°), which represents the time-averaged direction is marked "x" and used as the reference direction. Samples from MGD-A-E, MGD-H-I, and MGD-J have directions grouped near the GAD direction. Other samples (from MGD-G, IBW, and MCW) display a different pattern of scatter that falls outside the expected range of the geomagnetic field direction. Fisher means of these three sites yield $\alpha_{95} > 15$ and therefore rejected from further analyses. These results show that (1) the standing wall (MGD-A-E) was most probably heated in the position as it was found, (2) some collapsed bricks and wall segments (MGD-H-I, MGD-J) were still hot after they fell, and (3) some collapsed bricks and wall segments (MGD-G, IBW, MCW) were heated and cooled down before they fell.

To best calculate a mean archaeomagnetic direction representing the geomagnetic field at the time of the fire that engulfed Level Q-7, we plot in Figure 5b wall segments with directions grouped near the GAD (MGD-A-E, MGD-H-I, MGD-J) and calculate the Fisher statistics of the possible combinations from these segments (Table 3). Samples from wall segments MGD-A-E and MGD-H-I are clustered together, and the α_{95} cone of the two segments overlap. The four samples from brick MGD-J, however, are more scattered and fall outside the α_{95} cones of MGD-A-E and MGD-H-I. A comparison of the α_{95} and k calculated from these wall segments (Table 3) shows that k is highest for segment
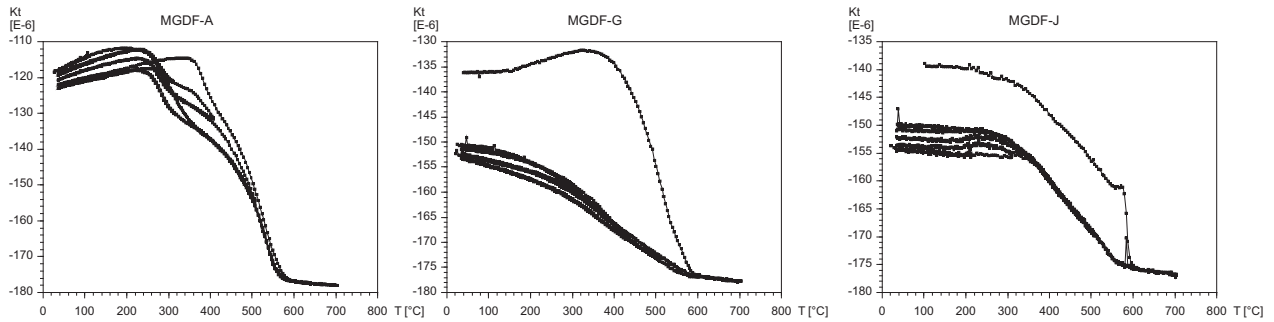
MGD-A-E ($n = 14$, $k = 135$, $\alpha_{95} = 3.4$), and α_{95} is lowest when samples from MGD-A-E and MGD-H–I are merged into one archaeomagnetic site, labeled "MGD-A-E, H-I," hereafter ($n = 21$, $k = 104$, $\alpha_{95} = 3.1$). If segment MGD-J is added to the site mean calculation (MGDA-E,H-I,J), k decreases and α_{95} increases ($n = 25$, $k = 74$, $\alpha_{95} = 3.4$). We therefore conclude that MGD-A-E and MGD-H-I are indistinguishable and consider the site mean of "MGD-A-E, H-I" as best representing the reference geomagnetic field direction at the time of the fire.

Figure 5c shows an equal area projection with four Fisher means of four archaeomagnetic sites: "MGD-A-E, H-I" (fired wall segments in Level Q-7), "MTQK" (cooking oven on the Q-7 floor), "MGDF" and "CWV" (burnt standing wall segments outside area Q with unknown stratigraphic affiliation); for field positions, see Figures 1 and 3. The overlap of the α_{95} confidence cones of "CWV" and "MGD-A-E, H-I" indicates that the heating event of these walls can be contemporaneous. Similarly, the overlap of the α_{95} cones for MGDF and MTQK would be consistent with these features having been heated at the same time; but, given the low number of samples ($n = 5$) and the high α_{95} of MTQK ($\alpha_{95} = 9°$), the archaeomagnetic site mean of MTQK is unreliable and should be taken with caution. The α_{95} confidence cones of "MGD-A-E, H-I" and CWV do not overlap with that of MGDF, indicating that it is very unlikely that MGDF represents the same age as the other two wall segments.

3.2 | Magnetic susceptibility

Figure 6 shows high-temperature susceptibility measurements of three representative samples from wall MGDF. Any difference between the heating and the cooling curves would indicate chemical alteration of the magnetic minerals upon heating. All samples show

FIGURE 6 High temperature magnetic susceptibility measured at progressively elevated peak temperature. Sample MGDF-A shows progressive alteration, while samples MGDF-G and MGDF-J show light alteration at low temperature and significant increase on cooling from 700°C. The alteration in the laboratory between 600°C to 700°C can be attributed to ancient heating temperature below 700°C.

perfectly reversible curves, with no alteration upon heating to 200°C and 300°C. Sample MGDF-A shows small, gradually increased alteration from 400° to 700°C. Samples MGDF-G and MGDF-J show minor and insignificant alteration between 400° and 600°C, but a significant change in susceptibility is observed between 600°C and 700°C. In all three samples, the dominant magnetic remanence carrier is likely to be magnetite, with Curie temperature of 585°C. Overall, differences in reversibility within this wall segment indicate heterogeneous heating of the whole segment or heterogeneous magnetic properties of raw materials for different bricks.

3.3 | Micromorphology and FTIR spectroscopy of burnt mud bricks

Mud bricks in Level Q-7 are composed of a silty-clay soil groundmass that includes pedogenic calcite nodules mixed with sand to gravel size particles including carbonaceous rock fragments (chalk and limestone), and occasional flint, basalt, ceramic, slag, bone, and shell fragments. Despite low amounts of bone fragments, their composition includes 2–3% of carbonated hydroxylapatite, a phosphate mineral often found in ash waste (Forget et al., 2015).

The structure of sun-dried mud bricks is massive, including abundant planar voids, which are pseudomorphic after chaff temper (Friesem et al., 2014). We observe this structure in black and beige-colored mud bricks (Table 4; archaeomagnetic site IBW). The infrared spectrum obtained from these bricks shows that the clay mineral component is unaffected by heat, that is, these bricks have not been heated above 500°C (Table 4; archaeomagnetic site IBW), but may have been heated to a lower temperature. The groundmass of these mud bricks is highly birefringent due to the calcitic nature of the parent soil material, and primary calcite is abundant (Figure 7a,b).

Mud bricks in the colors brown, yellow, and pinkish-red, from archaeomagnetic sites IBW, MGD-A-E, and MGD-G, have different micromorphological properties. Their groundmass is predominantly opaque, and there is a mixture of primary and secondary calcite, with the latter often found as void infilling (Figure 7c,d). FTIR spectroscopy results suggest that these mud bricks have been fired at a temperature range of 500–700°C (Table 2). Deeply red mud bricks (from archaeomagnetic site MGD-J) have also been fired at this temperature range, having some primary calcite present; however, their groundmass is

rubefied and not all of their voids are infilled with secondary calcite, suggesting that these bricks have been prepared from materials that have low amount of primary calcite to begin with (Figure 7e,f).

Mud bricks in the color of light yellow or yellow-white, from archaeomagnetic sites MGD-J and MGDF, show the most extreme deviation in structure and composition from unburnt mud bricks. Their groundmass is isotropic and secondary calcite is dominant. Voids are scarce, indicating structural collapse and sintering (Figure 7g,h). FTIR analysis of these bricks indicates exposure to temperatures around 700–800°C (Table 2) and a possible formation of new high-temperature mineral phases (yet to be identified).

4 | DISCUSSION

We present here an archaeomagnetic study of mud bricks and wall segments associated with a massive destruction event that occurred during the Late Iron Age I in Tel Megiddo. The method is used to reveal the temporal relation between the fire and the collapse in an urban context. Also, we use archaeomagnetism to address the question whether or not construction methods in Late Iron Age I at Tel Megiddo (Level Q-7) included preheated mud bricks. Although the study is conducted in a specific site in the Near East, its methodological implications are global and the approach can be applied at any site built from mud bricks across the world.

Field and micromorphological observations show that the Iron Age mud bricks under study are heterogeneous, composed of a variety of minerals at various grain sizes, as well as rock fragments and remains of human activity such as ceramics, bones, and slag fragments (Figures 3c and 7). Based on FTIR analysis, mud bricks have been heated to a range of temperatures from below 500°C to around or above 800°C. The results of this study demonstrate that fired mud brick walls can be valuable *in situ* archaeomagnetic recorders.

4.1 | Deciphering the construction method

Distinguishing construction with sun-dried mud bricks from construction with pre-fired bricks is fundamental for understanding destruction events. We address this through reconstruction of brick heating, based on demagnetization analysis, high-temperature susceptibility cycles,

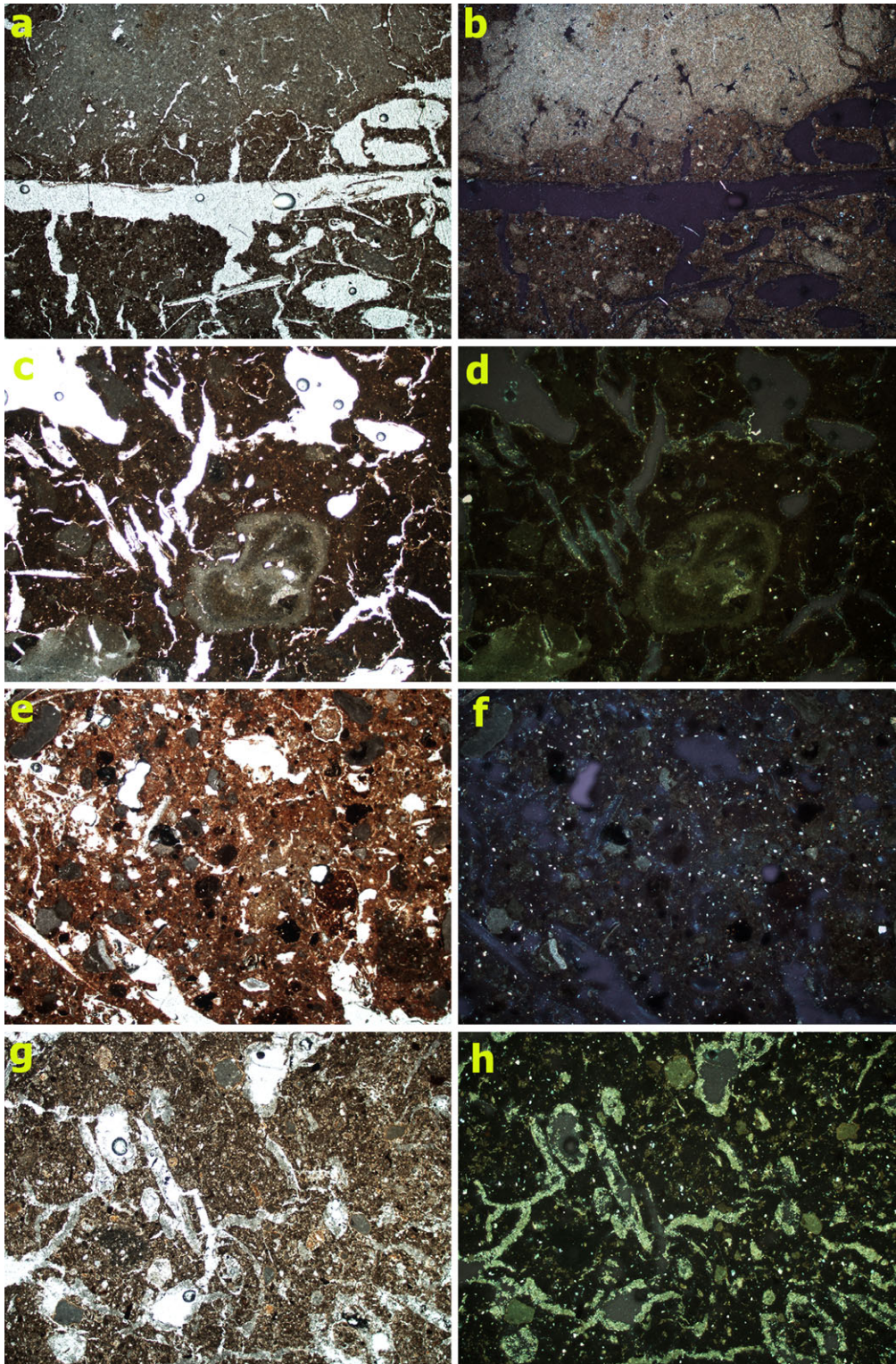**TABLE 4** Micromorphology of mud bricks from Level Q-7[a]

Sample number (archaeomagnetic site)	Field color	Groundmass b-fabric[b]	Planar voids[c]	Primary calcite (in XPL)	Pedofeatures
14/Q/056/LB 50 (IBW)	Yellow edge	Dull crystallitic	Few, filled	Blackened nodules; white with high relief	Micritic calcite infilling voids
	Brown inside	Dull crystallitic	Few, filled	Unaffected; blackened shell	Micritic calcite infilling voids
	Black core	Bright crystallitic	Many, open	Unaffected	None
14/Q/068/LB 22, 23 (IBW)	Light yellow	Isotropic	Few, filled	Unaffected; white with high relief	Micritic calcite infilling voids
14/Q/068/LB 27 (IBW)	Brown	Dull crystallitic	Many, open	Unaffected; blackened shell	None
14/Q/068/LB 24, 25 (IBW)	Pinkish-red	Rubefied	Few, open and filled	Unaffected; white with high relief	Micritic calcite infilling voids
14/Q/068/LB 29 (IBW)	Black	Bright crystallitic	Few, open	Unaffected	None
14/Q/068/LB 31 (IBW)	Beige	Bright crystallitic	Many, open	Unaffected; blackened shell	None
14/Q/068/LB 32 (IBW)	Beige-black	Bright crystallitic	Many, open	Unaffected; blackened shell and nodules; white with high relief	Root channels
14/Q/089/LB 12, 13	Yellow-white	Isotropic	Few, filled	White with high relief	Collapse of structure, almost no voids
12/Q/204 (MGD-A-E)	Yellow	Isotropic	Many, filled	Unaffected; blackened shell; white with high relief	Micritic calcite infilling voids; root channels
12/Q/184 (MGD-G)	Yellow part	Isotropic	Few, filled	White with high relief	Micritic calcite infilling voids
	Pinkish-red	Dull crystallitic	Few, filled	Unaffected; blackened shell	None
12/Q/184 (MGD-J)	Reddish-brown	Bright crystallitic	Many, filled	Unaffected; blackened shell	Micritic calcite infilling voids; root channels
12/Q/205 (MGDF)[a]	Yellow-white	Isotropic	Few, filled	Unaffected; blackened shell; white with high relief	Collapse of structure, almost no voids

[a] Samples from wall MGDF are not associated to Level Q-7.

[b] Dull crystallitic: slightly birefringent, i.e., some calcite is present; bright crystallitic: highly birefringent, i.e., groundmass is highly calcitic; isotropic: no birefringence, i.e., no calcite in the groundmass; rubefied: deeply red groundmass having high relief.

[c] Open: clearly visible planar voids without infilling; filled: planar voids sometimes having undulating and diffused edges, filled with secondary calcite.

Different colors suggest different firing conditions (e.g., temperature, duration, oxygen level) and/or differences in original material composition. Primary carbonates are present in the form of pedogenic calcite nodules, chalk, limestone, and aragonitic shell fragments. Secondary calcite is present in the form of micritic calcite in voids, expected to form following re-carbonation after burning at temperatures close to or higher than 600°C.

FIGURE 7 Micromorphological characteristics of mud bricks from Level Q-7. (a) Black mud brick, fired to less than 500°C, showing microstructure and groundmass properties similar to that of sun-dried mud bricks, i.e., silty-clay groundmass with open planar voids after chaff temper. Plane polarized light (PPL). (b) Same, in crossed polarized light (XPL). Note the highly crystallitic b-fabric. (c) Yellow mud brick, fired at ca. 500–600°C, PPL. Note the blackened calcite nodule, presence of unaffected calcitic fragments, and open planar voids. (d) Same, in XPL. Note the dull crystallitic b-fabric. (e) Red mud brick, fired at ca. 500–600°C, PPL. Note the rubefied appearance of the groundmass and presence of open voids. (f) Same, in XPL. Note the dull crystallitic b-fabric. (g) Yellow-white mud brick, fired at ca. 700–800°C, PPL. Note the shattered appearance of the groundmass. (h) Same, in XPL. Note the isotropic appearance of the groundmass and dominance of secondary calcite infilling voids. The width of view in all photomicrographs is 7.2 mm [Color figure can be viewed at wileyonlinelibrary.com]

clay mineral infrared spectrum, micromorphology, and field observations.

Demagnetization: If the bricks were pre-fired, and then heated again during conflagration to a lower temperature, below the maximal T_B of the material, we would expect to identify two magnetization vectors in the demagnetization experiments pointing to different directions. Both the AF and the thermal demagnetizations showed a single magnetization vector in all samples ruling out this option. Thermal demagnetization analysis on one brick from wall MGDF (Figure 5b) indicates that this brick was exposed to at least 590°C. This puts a lower bound for the maximal heating temperature of wall MGDF. Hence, it is possible that the last heating of the bricks exceeded the Curie temperature of magnetite (585°C), thus erasing any previous magnetization that may have been acquired if pre-firing took place. From FTIR analysis, we infer that other bricks in this wall were heated to temperatures near, or even exceeding, the T_c of magnetite. Thus, we suggest that the last heating event, during the destruction event, masked potential previous magnetic signal/s. Therefore, in the case of wall MGDF, we cannot rule out the possibility that the bricks were pre-fired before they were used in construction.
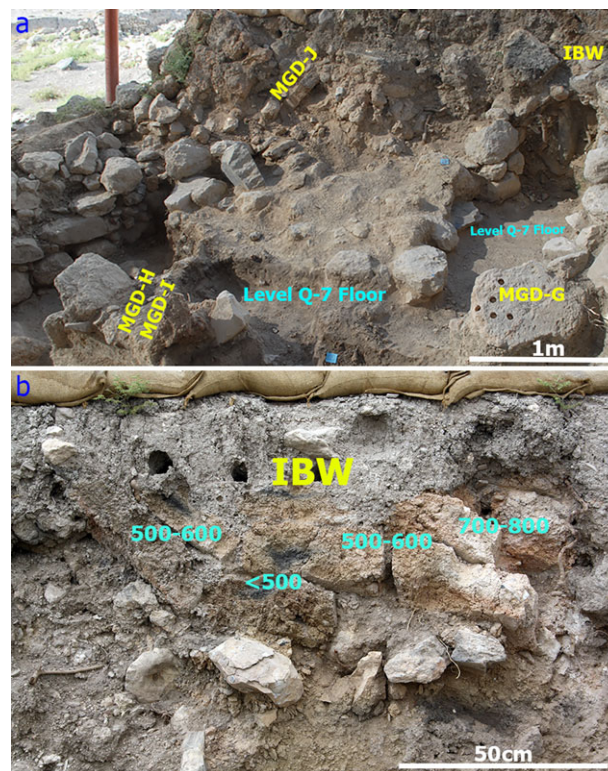
High-temperature susceptibility: These measurements, also conducted on bricks from wall MGDF, help put an independent bound to the temperature mud bricks have been heated to. The difference in heating and cooling curves indicates a change in the magnetic mineralogy between 600°C and 700°C. We suggest that this signal indicates that the ancient heating did not surpass 700°C.

FTIR, micromorphology, and field observations: The maximum heat reconstructed for wall MGDF using magnetic susceptibility (700°C) fits well with the reconstruction to a maximum of 700–800°C using clay mineralogy via FTIR spectroscopy. This is also supported by micromorphological criteria. It is therefore safe to use FTIR and micromorphology criteria together with archaeomagnetic direction data to understand the method of construction of walls studied in Level Q-7.

Taken together, based on FTIR and micromorphology, mud bricks from the standing *in situ* wall MGD-A-E have been heated to 500–600°C, and all of them have similar archaeomagnetic directions pointing roughly toward the reference geomagnetic field. This indicates that the whole wall was heated as a single unit. The collapsed wall IBW is the only wall that was studied in section where it was observed that it is composed of a highly fired edge (*ca.* 700–800°C) and a blackened core that was exposed to temperatures below 500°C (Figure 8). Forget et al. (2015) argued that this pattern too indicates that the wall was heated as a single unit, and that the temperature gradient indicates construction from sun-dried mud bricks. Together, the data from walls MGD-A-E and IBW argue in favor of construction with sun-dried mud bricks, which were then heated after wall construction. This suggestion is supported by the lack of brick kilns in or outside Megiddo, despite surveys and excavations in the area for over a century.
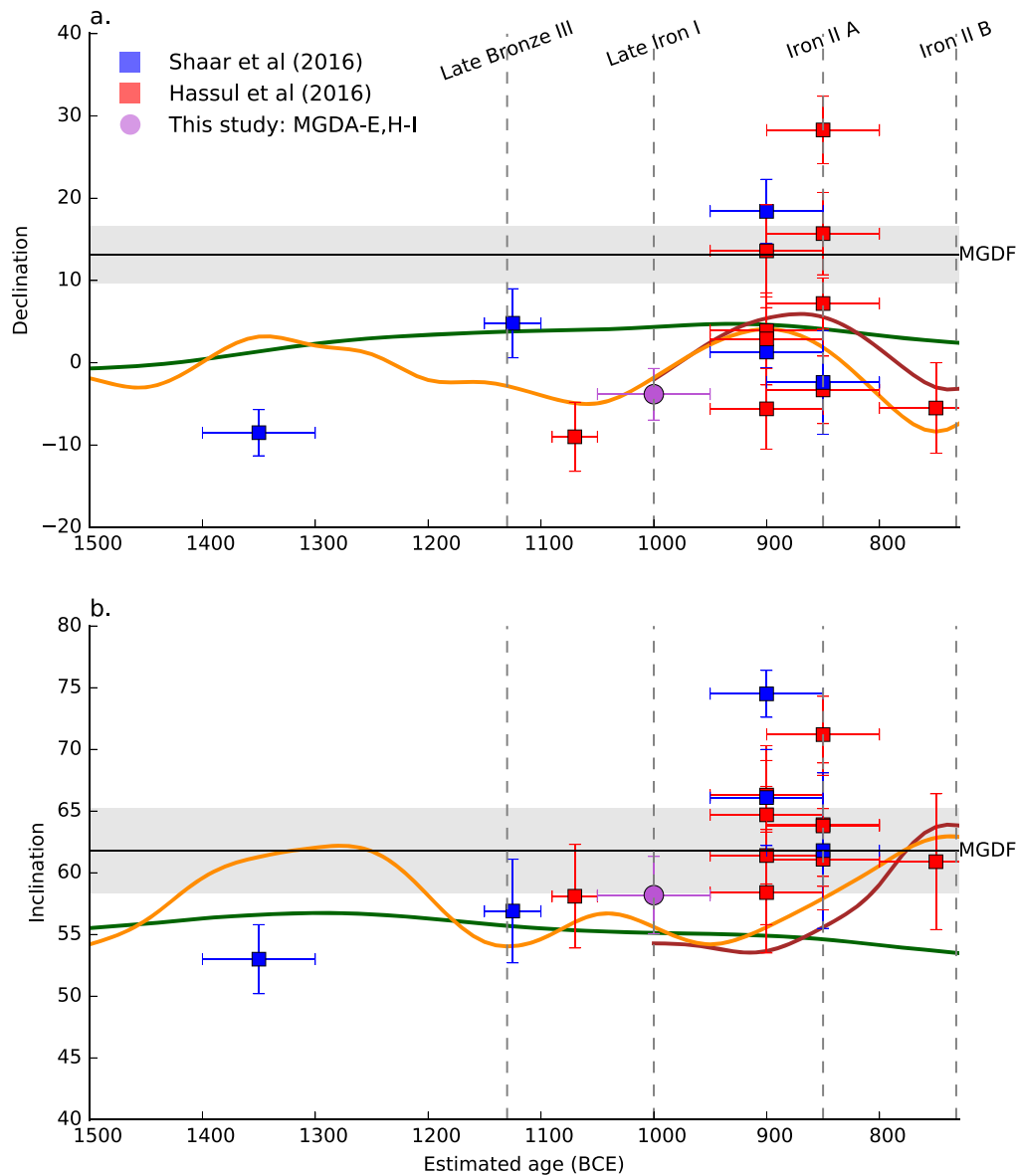
4.2 | Reconstructing directions of architectonic collapse

The archaeomagnetic site mean of the *in situ* standing wall segment MGD-A-E serves as an "anchor" for the geomagnetic field direction at

FIGURE 8 (a) General view of excavation square I/2 (looking north), showing location of archaeomagnetic sites of wall segments. The blackened floor of Level Q-7 can be appreciated, and the placement of the mud bricks above the floor, forming the destruction debris. (b) Close up on a section through wall IBW, with annotation of the heat (in °C) recorded by clay minerals via FTIR analysis as well as brick micromorphology. Note the temperature gradient across the wall section and the blackened area in its core where heat did not surpass 500°C [Color figure can be viewed at wileyonlinelibrary.com]

the time of the fire in Level Q-7. Directions of samples from collapsed bricks that cluster around this anchor direction indicate that architectonic features burnt following their collapse, while scattered archaeomagnetic directions of a certain archaeomagnetic site would indicate that architectonic features burnt in another position than the one they are found in. We have examples of both possibilities. Wall segment MGD-H-I is composed of two mud bricks that form a part of a tilted (i.e., collapsed) wall (Figure 3d). The archaeomagnetic directions obtained from both mud bricks cluster near those of MGD-A-E. This indicates that wall segment MGD-H-I cooled down as a single unit, after collapsing to the position in which it was found during the excavation. Samples from the single-brick MGD-J show scattered archaeomagnetic directions falling close to the "anchor" direction of MGD-A-E, indicating it too cooled down in the location it was found in the excavation. The bricks from collapsed segments MGD-G, IBW, and MCW show a totally different archaeomagnetic direction, probably indicating that they collapsed after cooling down in another position. Overall, we show here evidence for the variety of collapse possibilities during destruction by fire—walls remaining in place, walls collapsing while hot or first collapsing and then burning, and walls burning, cooling down, and then

FIGURE 9 Archaeomagnetic dating of wall MGDF using declination (a), and inclination (b) directions obtained from 15 cooking ovens in Tel Megiddo (Shaar et al., 2016, Hassul et al., in press) and from Q-7 archaeomagnetic site MGD-A-E, H-I (this study). Vertical dashed lines mark four known destruction events in Tel Megiddo. Solid lines show directions in Tel Megiddo calculated from models pfm9k (Green line; Nilsson et al. 2014), SHA.DIF.14k (orange line; Pavón-Carraso et al., 2014), and ARCH3k.1 (brown line; Korte et al., 2009). The horizontal gray stripe is the direction of MGDF that best matches directions recorded in the Iron Age IIA destruction event. [Color figure can be viewed at wileyonlinelibrary.com]

collapsing. This is a unique contribution to understanding collapse patterns in Near Eastern destruction layers.

4.3 | Archaeomagnetic dating of burnt walls

Of the three standing walls studied here, only wall MGD-A-E from Level Q-7 has a well-defined chronological affiliation, that is, the Late Iron Age I (*ca.* late eleventh to early tenth century B.C.E.). Archaeomagnetism can be used to assign the most likely chronostratigraphic affiliation to the two burnt walls found outside Area Q that were left standing after the 1930s excavations (CWV, MGDF) by comparing their archaeomagnetic data with that available from the region. The extent to which the TRM of Q-7 MGD-A-E agrees with Late Iron

Age I data for the geomagnetic field during that time window serves as a test for the present approach. A robust continuous archaeomagnetic curve for the Levant is not yet in hand. Yet, our on-going archaeomagnetic study in Tel Megiddo has yielded so far 15 archaeomagnetic directions that can be used as a basis for dating. Figure 9 shows archaeomagnetic directions obtained from 15 cooking ovens in Tel Megiddo (Hassul et al., in press; Shaar et al., 2016) as well as the direction of "MGD-A-E, H-I," the anchor for Level Q-7 dated to the Late Iron Age I, and directional variations expected in Tel Megiddo calculated from three different global geomagnetic models (Korte, Donadini, & Constable, 2009; Nilsson, Holme, Korte, Suttie, & Hill, 2014; Pavón-Carrasco, Osete, Torta, & De Santis, 2014). Because of the low density of the Levantine archaeomagnetic data in the global

data sets used to construct the above geomagnetic models, all showing a smoothed-out behavior, there are differences between the models and the Tel Megiddo data. Yet, the models predict quite well the trends shown in Tel Megiddo. Figure 9 shows the four known destruction events in Tel-Megiddo (Finkelstein & Piasetzky, 2009) as vertical dashed lines. We assume that wall MGDF was burnt in one of these events. By comparing the declination and inclination from MGDF (shown as a horizontal gray stripe in Figure 9) and the available data from Tel Megiddo, we can conclude at a reasonable confidence that MGDF was heated during the Iron IIA destruction (*ca*. mid-ninth century B.C.E.). However, we stress that more archaeomagnetic data are required in order to build a robust data set that could enable a more precise and reliable archaeomagnetic dating.

Wall segment MGDF is found outside Area Q at a topographic elevation that is higher than that of Level Q-7. It has been exposed since the excavations conducted by the University of Chicago Expedition in the 1930s. Its elevation indeed fits the Iron Age IIA remains excavated in Area K in its immediate vicinity (Lehmann, Killebrew, & Gadot, 2000). The Iron Age IIA settlement represented by Stratum VA-IVB at Megiddo was at least partially destroyed by fire (Lamon & Shipton, 1939, p. 6, Figure 11, taken *ca*. 35 m to the north of wall segment MGDF). Thus, the independent archaeomagnetic interpretation of an Iron IIA affiliation for MGDF is in agreement with the archaeological site stratigraphy.

Wall segment CWV is found further away from Area Q, also left after the excavations carried out by the University of Chicago Expedition in the 1930s. It is built over by the city wall of Stratum IVA of the Iron IIB (first half of the eighth century B.C.E.). The archaeomagnetic directions of mud bricks from this wall (dec = 349, α_{95} = −11, inc = 61, α_{95} = 5.2; Table 3) overlap with those of wall segments MGD-A-E and H-I (Figure 5c), but also marginally overlap with the available declination/inclination data from the four known destruction events in Tel-Megiddo (*cf*., Table 3 and Figure 9). In this case, we cannot safely assign an archaeomagnetic age to this wall.

4.4 | Historical and anthropological implications

The data provided in this article are not merely for methodological demonstration. Even from this relatively small data set, several immediate anthropological inferences can be made. First, we demonstrate (based primarily on field observations, FTIR, and micromorphology) that in all likelihood, the walls in Level Q-7 were constructed using sun-dried mud bricks. This bears implications for the level of labor organization associated with construction at this Late Iron Age I city, as it required less effort and organizational skills than in the case of mass production of pre-fired mud bricks. The latter requires skilled personnel not only in the preparation of bricks but also in construction and use of brick kilns. Moreover, operation of brick kilns for the mass production of mud bricks would require large amounts of fuel, which arguably would have severe effects on the environment. As mentioned above, currently there is no evidence for brick kilns—of any period—in the region. It is possible to explain the results in this study as construction with sun-dried mud bricks and purposeful firing of walls before habitation (rather than destruction by fire); however, we find

this option unlikely because fuel requirements in a region that is not densely wooded will make this investment economically demanding and environmentally damaging.

From a historical perspective, the cause of destruction of Late Iron Age I Megiddo is still debated. While we cannot supply here conclusive evidence to support either destruction by an earthquake or by a conquest, we assume that a very large amount of combustibles would be required to bake entire walls. Whether these combustibles are present in an inhabited city or brought from the outside specifically to set the city on fire is a question for further research.

5 | CONCLUSION

The study demonstrates how archaeomagnetic analysis of fired mud bricks from *in situ* and collapsed wall segments can contribute to the understanding of ancient construction methods. This analysis also enables reconstruction of the manner by which walls collapse during a conflagration event. Finally, archaeomagnetic analysis proposes that chronostratigraphic correlations may be constrained using burnt walls. We recommend using multiproxy data, as demonstrated in this study, to evaluate heating temperatures. We then stress the importance of working with *in situ* standing wall segments, preferentially those cut through so that thermal gradients across walls could be appreciated. On a broader perspective, this study contributes to the growing tool-kit by which site formation processes can be approached and disentangled.

ORCID

Ruth Shahack-Gross http://orcid.org/0000-0001-8085-9381

REFERENCES

Ben-Yosef, E., & Ron, H. (in press). Reconstructing a seismic destruction at Tel Rehov: Insights from a paleomagnetic fold test on tilted walls in Area C, Stratum V. In A. Mazar & N. Panitz-Cohen (Eds.), *The Excavations at Tel*

Rehov 1997–2012 (Qedem Monographs Series). Jerusalem: Institute of Archaeology, The Hebrew University of Jerusalem.

Cline, E. H. (2011). Whole lotta shakin' going on: The possible destruction by earthquake of Stratum VIA at Megiddo. In I. Finkelstein & N. Na'aman (Eds.), *The Fire Signals of Lachish: Studies in the Archaeology and History of Israel in the Late Bronze Age, Iron Age, and Persian Period in honor of David Ussishkin* (pp. 55–70). Winona Lake, Indiana: Eisenbrauns.

Driessen, J. (2013). *Destruction: Archaeological, philological and historical perspectives*. Louvain-la-Neuve: Presses universitaires de Louvain.

Finkelstein, I. (2003). City states and states: Polity dynamics in the 10th–9th centuries B.C.E. In W. G. Dever & S. Gitin (Eds.), *Symbiosis, symbolism and the power of the past: Canaan, Ancient Israel, and their neighbors* (pp. 75–83). Winona Lake, Indiana: Eisenbrauns.

Finkelstein, I. (2009). Destructions: Megiddo as a case study. In D. J. Schloen (Ed.), *Exploring the Longue Durée: Essays in honor of Lawrence E. Stager* (pp. 113–126). Winnona Lake, Indiana: Eisenbrauns.

Finkelstein, I., & Piasetzky, E. (2009). Radiocarbon-dated destruction layers: A skeleton for Iron Age chronology in the Levant. *Oxford Journal of Archaeology*, 28, 255–274.

Finkelstein, I., Ussishkin, D., & Halpern, B. (2000). *Megiddo III*. Tel-Aviv: Monograph Series of the Institute of Archaeology Tel-Aviv, Tel-Aviv University.

Finkelstein, I., Ussishkin, D., & Halpern, B. (2006). *Megiddo IV: The 1998–2002 Seasons*. Tel Aviv: Monograph Series of the Institute of Archaeology Tel-Aviv, Tel-Aviv University.

Finkelstein, I., Ussishkin, D., & Cline, E. H. (2013). *Megiddo V: The 2004–2008 Seasons*. Tel Aviv: Monograph Series of the Institute of Archaeology, Tel Aviv University.

Fisher, R. (1953). Dispersion on a sphere. *Proceedings of the Royal Society of London*, 217A, 295–305.

Forget, M., Regev, L., Friesem, D., & Shahack-Gross, R. (2015). Physical and mineralogical properties of experimentally heated sun-dried mud bricks: Implications for reconstruction of environmental factors influencing the appearance of mud bricks in archaeological conflagration events. *Journal of Archaeological Science: Reports*, 2, 80–93.

Forget, M., & Shahack-Gross, R. (2016). How long does it take to burn down an ancient Near Eastern City? *Antiquity*, 90, 1213–1225.

Friesem, D., Karkanas, P., Tsartsidou, G., & Shahack-Gross, R. (2014). Where are the roofs? A geo-ethnoarchaeological study towards the identification of roofs in the archaeological record. *Archaeological and Anthropological Sciences*, 6, 73–92.

Gallet, Y., Genevey, A., Le Goff, M., Warmé, N., Gran-Aymerich, J., & Lefèvre, A. (2009). On the use of archeology in geomagnetism, and vice-versa: Recent developments in archeomagnetism. *Comptes Rendus Physique*, 10(7)630–648.

Goulpeau, L. (1994). Analyse archéomagnétique de structures en hypocauste. *Revue d'archéométrie*, 18(1), 43–51.

Harrison, T. P. (2004). *Megiddo 3: Final Report on the Stratum VI Excavations*. Chicago: Oriental Institute Publications.

Hassul, E., Shaar, R., Shahack-Gross, R., Nowaczyk, N., Finkelstein, I., & Agnon, A. (in press). Archaeomagnetic directions from burnt structures in Tel Megiddo. In I. Finkelstein & E. H. Cline (Eds.), *Megiddo VI*. Tel Aviv: Monograph Series of the Institute of Archaeology, Tel-Aviv University.

Homsher, R. S. (2012). Mud bricks and the process of construction in the Middle Bronze Age southern Levant. *Bulletin of the American Schools of Oriental Research*, 368, 1–27.

Kirschvink, J. L. (1980). The least-squares line and plane and the analysis of palaeomagnetic data. *Geophysical Journal International*, 62, 699–718.

Korte, M., Donadini, F., & Constable, C. G. (2009). Geomagnetic field for 0–3 ka: 2. A new series of time-varying global models. *Geochemistry, Geophysics, Geosystems*, 10, Q06008. doi: 10.1029/2008GC002297

Lamon, R., & Shipton, G. (1939). *Megiddo I: Seasons of 1925–34, Strata I-V*. Chicago: Oriental Institute Publications: University of Chicago Press.

Lanos, P., Kovacheva, M., & Chauvin, A. (1999). Archaeomagnetism, methodology and applications: Implementation and practice of the archeomagnetic method in France and Bulgaria. *European Journal of Archaeology*, 2(3), 365–392.

Lehmann, G., Killebrew, A., & Gadot, Y. (2000). In K. Area, I. Finkelstein, D. Ussishkin, & B. Halpern, & (Eds.), *Megiddo III* (pp. 123–139). Tel-Aviv: Monograph Series of the Institute of Archaeology, Tel-Aviv University.

Loud, G. (1948). *Megiddo II: Season of 1935–1939*. Chicago: Oriental Institute Publications.

Marco, S. (2008). Recognition of earthquake-related damage in archaeological sites: Examples from the Dead Sea fault zone. *Tectonophysics*, 453, 148–156.

Marco, S., Agnon, A., Ussishkin, D., & Finkelstein, I. (2006). Megiddo earthquakes. In I. Finkelstein, D. Ussishkin, & B. Halpern (Eds.), *Megiddo IV* (pp. 568–575). Tel-Aviv: Monograph Series of the Institute of Archaeology, Tel-Aviv University.

Namdar, D., Zukerman, A., Maeir, A. M., Katz, J. C., Cabanes, D., Trueman, C., … Weiner, S. (2011). The 9th century BCE destruction layer at Tell es-Safi/Gath, Israel: Integrating macro- and microarchaeology. *Journal of Archaeological Science*, 38, 3471–3482.

Nilsson, A., Holme, R., Korte, M., Suttie, N., & Hill, M. (2014). Reconstructing Holocene geomagnetic field variation: New methods, models and implications. *Geophysical Journal International*, 198, 229–248.

Pavón-Carrasco, F. J., Osete, M. L., Torta, J. M., & De Santis, A. (2014). A geomagnetic field model for the Holocene based on archaeomagnetic and lava flow data. *Earth and Planetary Science Letters*, 388, 98–109.

Regev, L., Cabanes, D., Homsher, R., Kleiman, A., Weiner, S., Finkelstein, I., & Shahack-Gross, R. (2015). Geoarchaeological investigation in a domestic Iron Age quarter, Tel Megiddo, Israel. *Bulletin of the American Schools for Oriental Research*, 374, 135–157.

Schumacher, G. (1908). *Tell el-Mutesellim I*. Leipzig: Haupt.

Shaar, R., Tauxe, L., Ron, H., Ebert, Y., Zuckerman, S., Finkelstein, I., & Agnon, A. (2016). Large geomagnetic field anomalies revealed in Bronze to Iron Age archeomagnetic data from Tel Megiddo and Tel Hazor, Israel. *Earth and Planetary Science Letters*, 442, 173–185.

Shaffer, G. D. (1993). An archaeomagnetic study of a wattle and daub building collapse. *Journal of Field Archaeology*, 20, 59–75.

Stevanović, M. (1997). The age of clay: The social dynamics of house destruction. *Journal of Anthropological Archaeology*, 16, 334–395.

Sternberg, R. S., & McGuire, R. H. (1990). Techniques for constructing secular variation curves and for interpreting archaeomagnetic dates. In J. L. Eighmy & R. S. Sternberg (Eds.), *Archaeomagnetic dating* (pp. 109–134). Tucson: University of Arizona Press.

Sternberg, R. S., Lass, E., Marion, E., Katari, K., & Holbrook, M. (1999). Anomalous archaeomagnetic directions and site formation processes at archaeological sites in Israel. *Geoarchaeology*, 14(5), 415–439.

Sternberg, R. S. (2008). Archaeomagnetism in archaeometry—A semicentennial review. *Archaeometry*, 50(6), 983–998.

Stoops, G. (2003). *Guidelines for analysis and description of soil and regolith thin sections*. Madison, Wisconsin: Soil Science Society of America Inc.

Tauxe, L., Shaar, R., Jonestrask, L., Swanson-Hysell, N. L., Minnett, R., Koppers, A. A. P., … Fairchild, L. (2016). PmagPy: Software package for paleomagnetic data analysis and a bridge to the Magnetics Information

Consortium (MagIC) Database. *Geochemistry, Geophysics, Geosystems, 17*, 2450–2463.

Torrence, R., & Grattan, J. (2002). The archaeology of disasters: Past and future trends. In R. Torrence & J. Grattan (Eds.), *Natural disasters and cultural change* (pp. 1–18). London: Routledge.

Twiss, K. C., Bogaard, A., Bogdan, D., Carter, T., Charles, M. P., Farid, S., … Yeomans, L. (2008). Arson or accident? The burning of a Neolithic house at Çatalhöyük, Turkey. *Journal of Field Archaeology, 33*, 41–57.

Van Beek, G. W., & Van Beek, O. (2008). *Glorious mud! Ancient and contemporary earthen design and construction in North Africa, Western Europe, the Near East, and Southwest Asia*. Washington, DC: Smithsonian Institute Scholarly.

Weiner, S. (2010). *Microarchaeology: Beyond the visible archaeological record*. Cambridge: Cambridge University Press.

Zarzecki-Peleg, A. (2005). Tel Megiddo during the Iron Age I and IIA-IIB: The excavations of the Yadin Expedition to Megiddo and their contribution for comprehending the history of this site and other contemporary sites in Northern Israel (Unpublished doctoral dissertation). The Hebrew University of Jerusalem, Jerusalem, Israel (in Hebrew).

Zijderveld, J. D. A. (1967). A.C. demagnetization of rocks: Analysis of results. In D. W. Collinson, K. M. Creer, & S. K. Runcorn (Eds.), *Methods in palaeomagnetism* (pp. 254–286). New York: Elsevier.

SUPPORTING INFORMATION

Additional Supporting Information may be found online in the supporting information tab for this article.